the macroscale, but observations of the micromechanisms are in effect equal in all the samples. This a typical fracture of ductile materials, usually named to cup and cone fracture. This form of ductile fracture occurs in stages that initiate after necking begins. First, small microvoids form in the interior of the material. Next, deformation continues and the microvoids enlarge to form a crack. In figure 5a is visible a planar zone that is the last who break, in figure 5b there in a migrograph of this zone and can be appreciated the presence of dimples. The described aspects are common to specimens produced in all the considered orientations. Overall, observations on the rupture surfaces suggest an extremely fine grain structure, which will be verified though observations on polished etched sections.

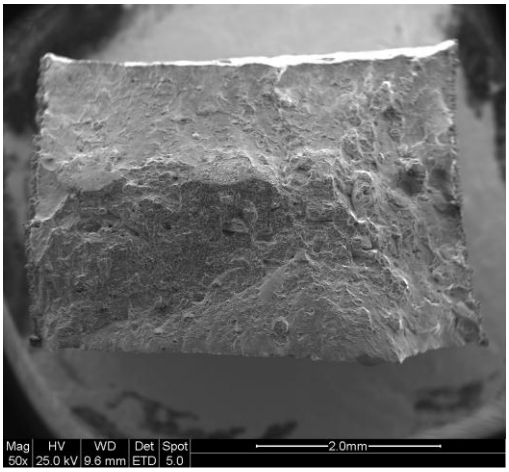

(a)

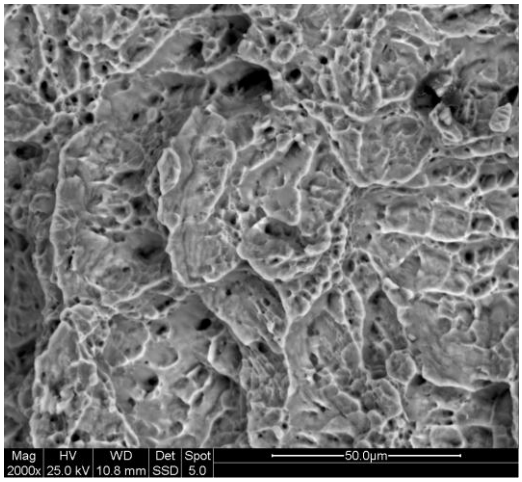

(b)

Figure 5a and 5b. Macro view and micrograph of a Ti specimen rupture surface.

Some cavities can be noticed on the rupture surfaces (Figure 5c), whose formation occurred during layer construction and indicated a balling phenomena [18]

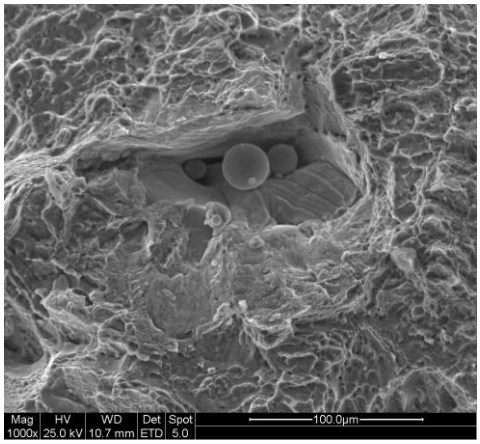

Figure 5c. Cavity on the rupture surface of a "0" specimen.

The rupture surface of CrCo specimens shows a uniform morphology across the section, shown in figures 6 . Failure seems to occur mainly by cleavage, even if the values of elongation at break would suggest a more ductile mode. In this cases can be used the term "quasi-cleavage", that indicate a fracture that has various amounts of transgranular cleavage but with evidence of plastic deformation.

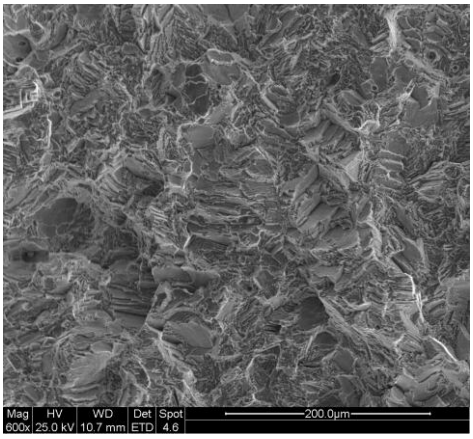

(a)

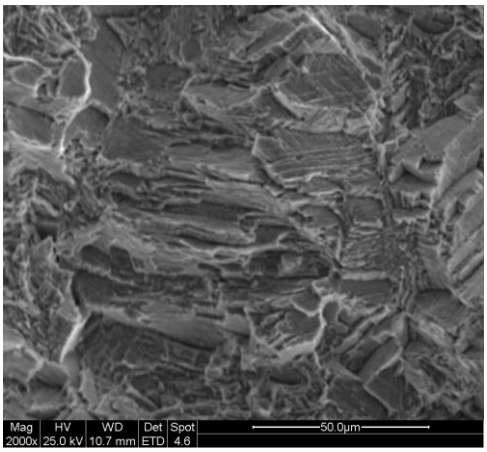

(b)

Figure 6a and 6b . Morphology of the rupture surface of Cr-Co specimens.

Observing the DMLS specimens it can be noticed that the different layers are no more visible, this indicates that the particles are strongly joined together not only within each layer but also between different layers. Isotropy in the build direction is a rarity in additive layer manufacturing techniques.

Porosity

Table 8 shows the results of the porosity calculation in the sections of the different specimens. In a preliminary phase samples were observed as a whole to assess the possibility of share the same in different areas, calculating for each of them porosity. The specimens revealed homogeneity.

Table 9: Porosity measured on specimens

SAMPLE	AVERAGE SIZE[μm²] Mean (dev. st.)	AREA FRACTION [%] Mean (dev. st.)
Ti 0	4.58 (6.092)	0.04 (0.074)
Ti 45	2.04 (0.552)	0.21 (0.064)
Ti 90	17.60 (11.318)	0.28 (0.225)
CoCr 0	15.87 (29.687)	0.55 (0.655)
CoCr 45	10.09 (8.856)	0.30 (0.214)
CoCr 90	18.78 (25.938)	0.43 (0.453)

The titanium specimens present a rather uniform porosity with an average size of pores contained, between 4 and 18 μm² and a low porosity that in under 0.3%. The t-test indicated that there is a significant difference in porosity due to orientation between Ti 0 and the others, but in percentage term the difference is contained in value of 0.2%.

The Cr-co specimen present a porosity that varies from 0.3% to near 0.55%, with an mean average size of pores between 10 and 20 μm². The t-test indicated that there is not a significant difference in porosity due to orientation

Table 10: p-value obtained by t-test on porosity results

	AVERAGE SIZE	POROSITY
Titanio 0° vs. Titanio 45°	0,26	0,00
Titanio 0° vs. Titanio 90°	0,01	0,01
Titanio 45° vs. Titanio 90°	0,00	0,46
Cromo 0° vs. Cromo 45°	0,61	0,32
Cromo 0° vs. Cromo 90°	0,84	0,66
Cromo 45° vs. Cromo 90°	0,38	0,49

Microstructure

The analysis of microstructure of titanium samples revealed that the tree orientation doesn't present difference. The specimen is homogeneous and exhibits the acicular α′ martensite microstructure, wich forms where the cooling rate is hight. In fact a rapid quenching leads to a martensitic transformation, leading to a very fine needle-like microstructure [19]. This kind of microstructure is difficult to obtain industrially and for this reason is not common

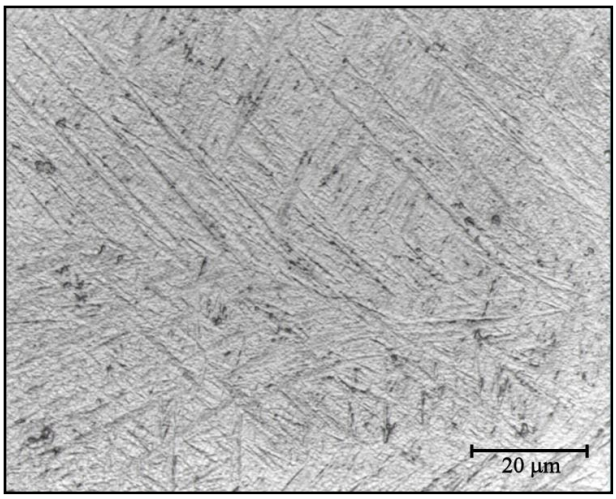

Figure 7: Micrograph of microstructure of Ti specimens

The Cr-co Specimens present a very particular macro-structure, like "fish scales", where the boundary are due to the melted zone by the laser. In fact all the semicircles are oriented in the same direction, that is growing one. Higher magnification shows a very fine acicular microstructure, where grain are oriented in different ways. The grains have a diameter lower than 1 μm as is visible in figure 8c and 8d. This fine structure is responsible of the performance of the material that are higher than those expected from bulk material.

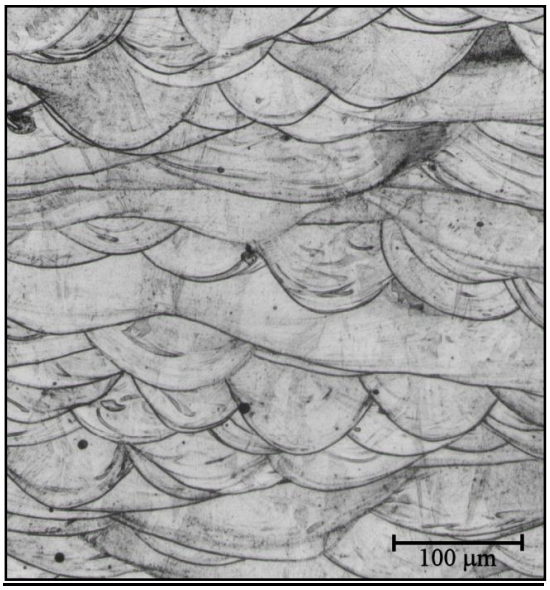

(a)

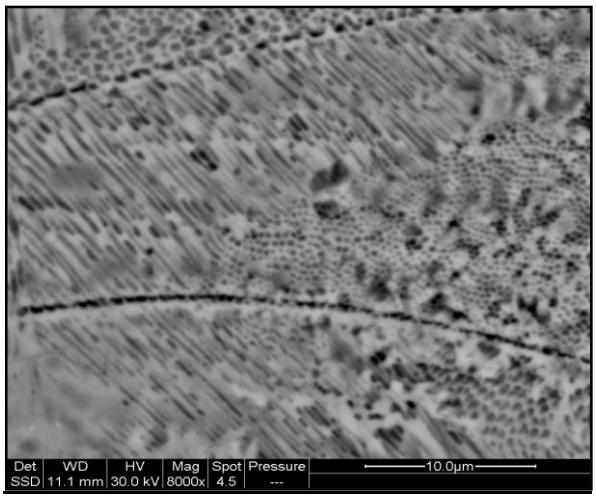

(b)

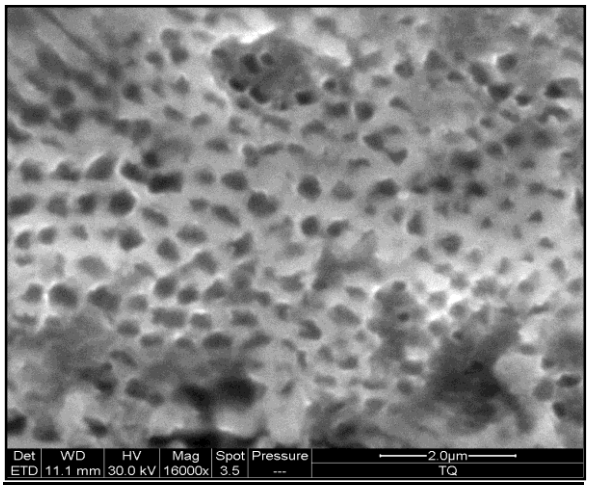

(c)

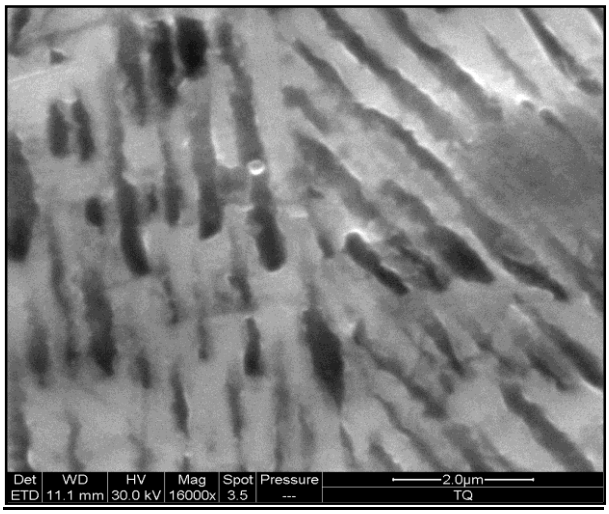

(d)

Figure 8a, 8b, 8c, 8d: Micrograph of microstructure of Cr-Co specimens

CONCLUSION

DMLS technique has been investigated comparing specimens built in different orientation in building camera, with two different dental alloy: Cr-Co and Ti6Al4V. Mechanical, physical, chemical and microstructural properties have been compared.

Both alloy produced by DMLS show high tensile strength, low porosity and high hardness. The physical and mechanical properties of the material mainly depend on its microstructure, so the observed very fine microstructure cause the macroscopic performances of the specimens. The microstructure of titanium specimens is a particular α' martensitic structure, whereas the Cr-Co show grain of the order of micrometers.

The statistic test does not indicate a unique difference between the building orientations, confronting all the results there are significant difference between group only in few cases and in these cases the numerical difference is very contained, as 30 MPa on 1100 MPa.

DMLS process is very reliable and repeatable; the experimental results show a very low standard deviation.

It can be concluded that, as to the possibility of using DMLS technology for the realization of prostheses in Cr-Co and Ti6Al4V alloy, from a mechanical point of view, the DMLS technique has good performance that does not depend from the orientation in the building camera.

REFERENCES

[1] Ashley S, "Rapid Prototyping is Coming of Age," Mechanical Engineering July 1995: 63

[2] Ashley S, "From CAD Art to Rapid Metal Tools," Mechanical Engineering March 1997: 82

[3] Bassoli E, Gatto A, Iuliano L. Joining mechanisms and mechanical properties of PA composites obtained by Selective Laser Sintering. RAPID PROTOTYPING JOURNAL, 2012 vol. 18 (2), p. 100-108

[4] Bassoli E, Gatto A, Iuliano L, Violante MG. 3D Printing technique applied to Rapid Casting.Rapid Prototyping Journal, 2007 vol. 13(3), p. 148-155,

[5] Glantz PO, Ryge G, Jendresen MD, Nilner K. Quality of extensive fixed prosthodontics after five years. J Prosthet Dent 1984;52:475-9.

[6] Walton TR. An up to 15-year longitudinal study of 515 metal-ceramic FPDs: Part 1. Outcome. Int J Prosthodont 2002;15:439-45.

[7] Laurell L, Lundgren D, Falk H, Hugoson A. Long-term prognosis of extensive polyunit cantilevered fixed partial dentures. J Prosthet Dent 1991;66:545-52.

[8] Eliasson A, Arnelund CF, Johansson A. A clinical evaluation of cobalt-chromium metal-ceramic fixed partial dentures and crowns: A three- to seven-year retrospective study. J Prosthet Dent. 2007 Jul;98(1):6-16.

[9] Tan K, Pjetursson BE, Lang NP, Chan ES. A systematic review of the survival and complication rates of fixed partial dentures (FPDs) after an observation period of at least 5 years. Clin Oral Implants Res 2004;15:654-66.

[10] Schmalz G, Garhammer P. Biological interactions of dental cast alloys with oral tissues.Dent Mater 2002;18:396-406.

[11] Al-Hiyasat AS, Bashabsheh OM , Darmani H. An investigation of the cytotoxic effects of dental casting alloys. Int J Prosthodont 2003;16:8-12.

[12] Andersson M, Oden A. A new all ceramic crown. A dense-sintered, high purity alumina comping with porcelain. Acta Odontol Scand 1993;51:59-64

[13] Richard Bibb, Dominic Eggbeer, Robert Williams, Rapid manufacture of removable partial denture frameworks, Rapid Prototyping Journal Volume: 12 Issue: 2 2006

[14] Maarten van Elsen, Farid Al-Bender, Jean-Pierre Kruth, (2008) "Application of dimensional analysis to selective laser melting", Rapid Prototyping Journal, Vol. 14 Iss: 1, pp.15 – 22

[15] Simchi A, Direct laser sintering of metal powders: Mechanism, kinetics and microstructural features Original Materials Science and Engineering: A, Volume 428, Issues 1-2, 25 July 2006, Pages 148-158

[16] Facchini L, Magalini E, Robotti P, Molinari A, Höges S, Wissenbach K, Ductility of a Ti-6Al-4V alloy produced by selective laser melting of prealloyed powders, Rapid Prototyping Journal Volume: 16 Issue: 6 2010

[17] Kruth, J.-P.; Mercelis, P.; Van Vaerenbergh, J.; Froyen, L.; Rombouts, M., Binding Mechanisms in Selective Laser Sintering and Selective Laser Melting, 2005, Rapid prototyping journal, Vol. 11, p.26-36

[18] Dongdong Gu, Yifu Shen, Balling phenomena in direct laser sintering of stainless steel powder: Metallurgical mechanisms and control methods, Materials & Design, Volume 30, Issue 8, September 2009, Pages 2903-2910

[19] H. Matsumoto, H. Yoneda, K. Sato, S. Kurosu, E. Maire, D. Fabregue, T. J. Konno, A. Chiba, Room-temperature ductility of Ti–6Al–4V alloy with α' martensite microstructure, Materials Science and Engineering A, Volume 528, Issue 3, 25 January 2011, Pages 1512-1520